Self-propulsion of droplets driven by chemical turnover

Deepti Kannan[1]

[1] *Department of Physics, Massachusetts Institute of Technology, Cambridge, Massachusetts 02139, USA*

(Dated: May 20, 2023)

Active droplets driven by chemical reactions are prevalent in living systems and exhibit rich dynamical phenomena. We study a minimal model of a phase-separating system where a protein species c, which follows conserved dynamics, catalyzes the production of an RNA species m according to a reaction diffusion equation. Closely following the analysis in Ref.[1], we find that droplets show a self-propulsion instability due to RNA concentration differences between the droplet interfaces. We outline an approach to self-consistently calculate the self-propulsion velocity in arbitrary dimensions. We then study the flow of 2D and 3D protein droplets in response to RNA concentration gradients generated by a localized source. Finally, we compare our 2D calculations to phase field simulations of the full nonlinear dynamics and find good agreement.

Membraneless compartments called biomolecular condensates are an important driver of cellular organization [2]. Condensates concentrate biomoleculues through a network of multivalent interactions and are thought to form via liquid-liquid phase separation [3]. In the cell, condensates are coupled to nonequilibrium reactions which can modulate their material properties. For example, transcriptional condensates can facilitate the production of nascent RNA by recruiting transcription factors and coactivators in a dense phase near an enhancer or gene locus [4]. Other examples of nuclear bodies that promote RNA production include nuclear speckles and the nucleolus, which organizes the synthesis of ribosomal RNA [3].

Condensates driven out of equilibrium via chemical reactions exhibit rich phenomena not present in thermal phase separating systems [5]. For example, fuel-driven reactions can arrest Ostwald ripening and lead to multidroplet coexistance [6]. More recent works have demonstrated that continuous turnover of droplet material can also lead to droplet division [7] and self-propulsion [1, 8]. The directed, superdiffusive motion of droplets has been realized experimentally in systems of active colloids via Marangoni flows [9]. Biomolecular condensates such as nuclear speckles [10] have also shown ballistic motion, although less is known about the mechanism of propulsion in living cells.

In order to understand how chemical turnover induces droplet flow, we study a phase field model of a conserved species $c(\boldsymbol{x}, t)$ (proteins) which can produce a nonconserved species $m(\boldsymbol{x}, t)$ (RNA). We assume that the conserved species can phase separate on its own according to a Cahn-Hilliard free energy (double well potential)

$$f_0(c) = u(c - c_0)^4 - r(c - c_0)^2 + \kappa|\nabla c|^2, \qquad (1)$$

where c_0 represents the critical protein concentration and κ is the surface tension. The interactions between positively charged proteins and negatively charged RNA are designed to exhibit a re-entrant phase transition. For a fixed protein concentration, electrostatic attraction at low values of m promotes phase separation, whereas an excess accumulation of negative charge at higher values of m repels protein material. Indeed, this complex coascervate behavior has been observed *in vitro* in RNA-protein mixtures [11]. All together, this implies a Landau-Ginzburg free energy of

$$\mathcal{F}(c, m) = \int d^d x \ \left[f_0(c) + \rho m^2 + \chi c m + \gamma c^2 m^2 \right]. \quad (2)$$

For the purposes of our analysis, we neglect the "re-entrant" term $\gamma c^2 m^2$.

The protein species obeys conserved Model B dynamics, whereas the RNA species obeys a reaction diffusion equation with a production rate that depends on the concentration of c:

$$\partial_t c = \boldsymbol{\nabla} \cdot [M_c(\boldsymbol{\nabla}\mu_0(c) + \chi \boldsymbol{\nabla} m)] \qquad (3a)$$

$$\partial_t m = D\boldsymbol{\nabla}^2 m + k_p c - k_d m. \qquad (3b)$$

Equations (3a) and (3b) represent a special case of the model studied in Ref.[1], in which an enzyme (analogous to c) catalyzes the conversion of substrate to product (analogous to m). The authors also included an enzyme mobility that depends on its concentration, $M(c) = M_c c$, but here we set both mobilities to be constant.

The steady state profiles of c and m are analytically solvable in the sharp interface limit where the interface width $\sqrt{2\kappa/r}$ is much smaller than all other length scales relevant to the dynamics. We further assume that interactions are weak, $|\chi m| \ll r(c_+ - c_-)$, such that the protein concentrations in the dense and light phases are given by their equilibrium values, $c_+ = c_0 + \sqrt{r/u}$ and $c_- = c_0 - \sqrt{r/u}$, respectively. In 1D, the resulting steady state profile for $c(x, t)$ is a step function centered at the origin, with value c_+ within $|x| \leq R$ and c_- otherwise, where R is the radius of the 1D droplet. We then calculate the steady state profile of m in response to this profile by solving the inhomogeneous Helmholtz equation on three domains (Fig. 1). Symmetry about the origin

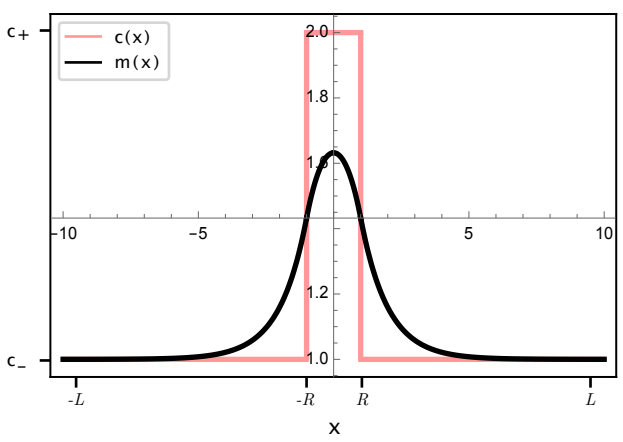

FIG. 1. Steady state protein $[c(x)]$ and RNA $[m(x)]$ concentration profiles for a droplet of radius $R = 1$ with no flux boundary conditions at $x = \pm L$. RNA profile is determined by a balance of reactive and diffusive fluxes, with diffusion length $l = \sqrt{D/k_d} = 1$, $k_p = 1$, $c_+ - c_- = 1$, $D = 1$, and $L = 10$.

implies the following functional form:

$$m(x) = \begin{cases} 2A\cosh\left(\frac{x}{\ell}\right) + \frac{k_p c_+}{D}\ell^2, & -R \le x \le R \\ Be^{|x|/\ell} + Ce^{-|x|/\ell} + \frac{k_p c_-}{D}\ell^2, & |x| > R \end{cases} \tag{4}$$

where the integration constants A, B, and C are determined by imposing no flux boundary conditions at the edges of the domain ($|x| = L$) and smoothness and continuity of the solution at the droplet boundary.

The protein droplet promotes production of RNA within the droplet, which is balanced by diffusion of RNA outside of the droplet, leading to a profile that decays exponentially with the characteristic diffusion length $\ell = \sqrt{D/k_d}$. In the limit of an infinitely large domain, $B \to 0$ and the RNA concentrations in the far field are given by their local reactive equilibria, $m(\pm\infty) = k_p c_-/k_d$. At the center of the droplet, the RNA concentration is shifted from its equilibrium value by an amount $\Delta m = 2A = e^{-R/\ell}(c_- - c_+)k_p\ell^2/D$. Thus, the shift depends on the relative size of the droplet compared to the diffusion length and is proportional to the enrichment of proteins relative to the surrounding solution.

Next, we investigate whether a difference in RNA concentration at the two droplet interfaces could drive droplet motion through a chemical potential gradient. To analyze the conditions for the onset of this self-propulsion instability, we follow the approach of Ref. [1] and use a traveling wave ansatz $c_{\text{sharp}}(x - vt) \equiv c(z)$ for the protein concentration profile. We then solve Eq. (3b) for the RNA profile in the co-moving frame $m(z)$, which amounts to solving the Helmholtz equation with a linear advection term $\partial_t m = -v\partial_z m(z)$ [solution in Fig. 2a].

In order to solve for the self-propulsion velocity, we

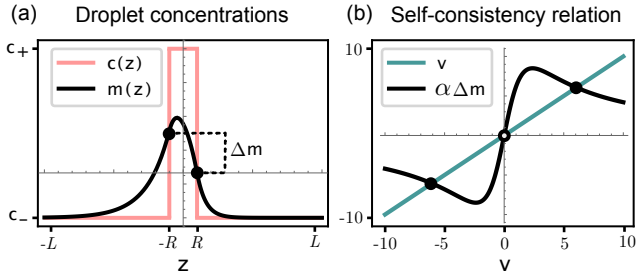

FIG. 2. (a) RNA concentration profile in the co-moving frame, $m(z \equiv x - vt)$, assuming a traveling wave solution for the protein droplet $c(z)$ with $v = 1$ and no flux boundary conditions at $x = \pm L$. (b) Self-consistency relation for the droplet velocity v, which can be extracted graphically as the intersection of v and $\alpha\Delta m(v)$, where $\Delta m = m(R) - m(-R)$ is the difference in RNA concentrate at the two droplet interfaces and $\alpha = -M_c\chi/[2R(c_+ - c_-)]$. We use the same parameters as in Fig. 1 with $M_c\chi = 20$.

analyze the continuity equation [Eq. (3a)] for the protein dynamics in the co-moving frame,

$$\partial_z\{M_c\partial_z[\mu_0(c(z)) + \chi m(z)]\} = -v\partial_z c(z) = -j(z). \tag{5}$$

Integrating Eq. (5) once, the right hand side becomes $-vc(z) + j_0$, where the integration constant $j_0 = vc_-$ is determined by noting that at $z = \pm\infty$ the concentration fields are homogeneous and $c(\pm\infty) = c_-$. Integrating Eq. (5) again from $-R$ to R and using the sharp interface approximation for $c(z)$ gives

$$v = -\frac{M_c\chi\Delta m(v)}{2R(c_+ - c_-)}. \tag{6}$$

Eq. (6) represents a self-consistency relation for the self-propulsion velocity v, which emerges from asymmetries in the RNA concentraion profile, $\Delta m = m(R) - m(-R)$. Note that our ansatz of droplet motion at a constant velocity implies that $\mu_0(R) - \mu_0(-R) = 0$, and thus the chemical potential drops out of Eq. (6).

The self-consistency relation, plotted in Fig. 2b, can be solved graphically and has a solution when

$$\begin{aligned} 1 &< -\left.\frac{M_c\chi}{2R(c_+ - c_-)}\partial_v\Delta m(v)\right|_{v=0} \\ &= \frac{M_c\chi k_p}{4Dk_d}\left[\frac{1 - (1 - 2R/\ell)e^{-2R/\ell}}{R/\ell}\right]. \end{aligned} \tag{7}$$

Eq. (7) defines a critical point for the onset of droplet flow, where the control parameters are the ratio of the protein and RNA mobilities and the ratio of the RNA production and degradation rates. The dimensionless term in brackets is a non-monotonic function of R/ℓ, suggesting that the self-propulsion instability is suppressed for very large or very small droplets. When the droplet diameter is small, the RNA concentration difference between its interfaces is insufficient to generate motion. For

large droplets compared to the diffusion length, the RNA concentration in the droplet approaches its local reactive equilibrium value, which also implies a weak gradient across the droplet diameter. Thus, self-propulsion is enhanced when $R \sim \ell$.

DROPLET FLOW IN HIGHER DIMENSIONS

We now extend the 1D calculations to arbitrary dimensions by applying a theoretical framework developed by the same authors as in Ref. [1] (unpublished). To calculate the self-propulsion velocity self-consistently, we again analyze the continuity equation for $c(\boldsymbol{x} - \boldsymbol{v}t) \equiv c(\boldsymbol{z})$,

$$-\boldsymbol{v} \cdot \boldsymbol{\nabla} c(\boldsymbol{z}) = \boldsymbol{\nabla} \cdot [M_c(\boldsymbol{\nabla}\mu_0 + \chi \boldsymbol{\nabla} m(\boldsymbol{z})]. \tag{8}$$

As in 1D, we posit that in order for the droplet to exhibit steady motion with a constant velocity, the chemical potential $\mu_0(\boldsymbol{z})$ should be symmetric about the interface along the direction of flow $\hat{\boldsymbol{e}}_v$,

$$g(\boldsymbol{\nabla}\mu_0) = \int_{\mathcal{D}} d^d\boldsymbol{r} \;\; \hat{\boldsymbol{e}}_v \cdot \boldsymbol{\nabla}\mu_0 = 0, \tag{9}$$

where the domain $\mathcal{D}$ of integration is over the volume of the droplet, $|\boldsymbol{r}| \leq R$. If Eq. (9) does not hold, then the bare chemical potential would cause the droplet to accelerate or deccelerate. Thus, $g(\boldsymbol{\nabla}\mu_0)$ can be interpreted as a measure of the inconsistency of the proposed traveling wave solution which needs to be minimized (i.e. a Lagrange multiplier). By invoking the sharp interface approximation for $c(\boldsymbol{z})$ (round droplets in 2D or spherical droplets in 3D), one can solve Eq. (8) for $\mu_0(\boldsymbol{z})$ and then substitue into Eq. (9) to obtain a self-consistency relation for the droplet velocity $\boldsymbol{v}$.

Upon Fourier transforming Eq. (8) we find

$$\mu(\boldsymbol{r}) = \int \frac{d^d\boldsymbol{q}}{(2\pi)^d} \frac{i\boldsymbol{v}\cdot\boldsymbol{q}}{M_c q^2} c_q \mathrm{e}^{-i\boldsymbol{q}\cdot\boldsymbol{r}} - \chi m(\boldsymbol{r}), \tag{10}$$

where c_q is the Fourier transform of the droplet concentration field in the co-moving frame. Substituting Eq. (10) into Eq. (9), we find the following self-consistency relation for $\boldsymbol{v}$

$$-\int_{\mathcal{D}} d^d\boldsymbol{r} \frac{d^d\boldsymbol{q}}{(2\pi)^d} \frac{iv(\hat{\boldsymbol{e}}_v\cdot\boldsymbol{q})^2}{M_c q^2} c_q \mathrm{e}^{-i\boldsymbol{q}\cdot\boldsymbol{r}} = \chi \int_{\mathcal{D}} d^d\boldsymbol{r} \;\; \hat{\boldsymbol{e}}_v \cdot \boldsymbol{\nabla} m. \tag{11}$$

Eq. (11) shows that gradients in m can drive droplet motion in arbitrary dimensions via the coupling χ. If $\chi < 0$, the droplet will climb gradients in m, otherwise it will repel regions of high RNA concentration.

Flow of 3D droplets towards a point source

We now specialize to 3D and choose a coordinate system such that the droplet moves in the $\hat{\boldsymbol{z}}$ direction and

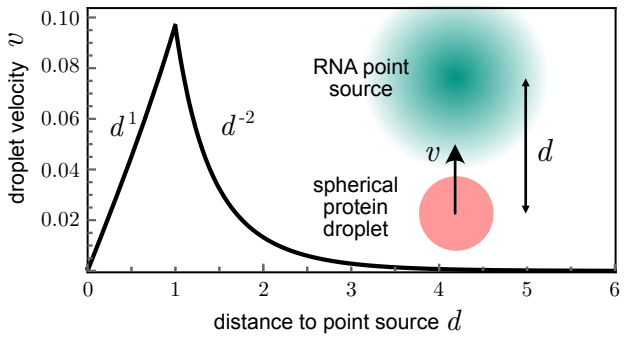

FIG. 3. Velocity of spherical droplet is non-monotonic in the distance to a point source of RNA production in 3D [Eq. (16)] for $R = \ell = 1$, $c_+ - c_- = 1$, $k_p = 1$, $M_c = 1$, and $\chi = -1$ (RNA attracts protein). Flow velocity is linear in d for small d, peaks at $d = R$, and decays as d^{-2}.

$\hat{\boldsymbol{e}}_v \cdot \boldsymbol{q} = q\cos\theta$. We further assume a spherical droplet with concentration c_- outisde the droplet and $c_- + \Delta c$ inside the droplet. Then

$$c_q = \int d^3\boldsymbol{z} c(\boldsymbol{z}) \mathrm{e}^{-i\boldsymbol{q}\cdot\boldsymbol{z}} = c_- \frac{\delta(q)}{4\pi q^2}(2\pi)^3 + \Delta c\, g(q), \tag{12}$$

where $g(q) = 2\pi \int_0^\pi sin\theta d\theta \int_0^R dr r^2 \mathrm{e}^{iqr\cos\theta}$. After integrating over θ in Eq. (11) and substituting c_q, we obtain

$$-\frac{2v}{3M_c}\left[\frac{c_-}{2} g(0) + \Delta c \int_0^\infty \frac{dq}{(2\pi)^2} q^2 g(q)^2\right] = \chi \int_{\mathcal{D}} \partial_z m, \tag{13}$$

where $g(0)$ is just the volume of the droplet. Integrating over q and applying the divergence theorem to the right hand side, we find that the self-propulsion velocity is given by a relatively simple expression

$$v = -\frac{3M_c\chi}{c_+(4\pi R^3/3)} \int_{\mathcal{S}} m(R,\theta)\cos\theta, \tag{14}$$

where the integral is over the surface of the spherical droplet, i.e. with integration measure $R^2 \sin\theta d\theta d\phi$.

We now investigate how a spherical droplet flows in response to a point source of RNA production a distance d away from the droplet centroid. To that end, we first solve the inhomogeneous Helmholtz equation in 3D for the RNA concentration profile,

$$m(\boldsymbol{r}) = \frac{k_p c_-}{4\pi D} \frac{\mathrm{e}^{-|\boldsymbol{r} - d\hat{\boldsymbol{z}}|/\ell}}{|\boldsymbol{r} - d\hat{\boldsymbol{z}}|}. \tag{15}$$

Here, we assume that RNA production only depends on the background concentration of protein c_- and is thus unaffected by the protein droplet. Of course, this assumption breaks down for $d < R$ since the droplet should stimulate RNA production at the source. Substituting

Eq. (15) into Eq. (14) and performing the integral gives

$$v = -\frac{3M_c\chi k_p c_-}{2c_+(4\pi R^3/3)D}\frac{l}{d^2}\left[e^{-\frac{R+d}{\ell}}(\ell+R)(\ell+d) - e^{-\frac{|R-d|}{\ell}}(\ell^2 - Rd + \ell|R-d|)\right]. \quad (16)$$

To gain insight into this expression, we consider the limit of infinite diffusion length $\ell \to \infty$ and find that the velocity is linear in d and inversely proportional to the droplet volume for $d < R$. The velocity is sharply peaked at $d = R$ and then falls off as d^{-2} for $d > R$ independent of the droplet radius [Fig. 3]. The large d behavior shows that away from the point source the droplet is simply sensing gradients in m which fall off as d^{-2} [c.f. Eq. (15)]. When $d = 0$, the droplet centroid and point source coincide and so the RNA concentration profile will be perfectly symmetric about the interface, causing motion to arrest. In the range $d \leq R$, the droplet starts to feel asymmetries in the RNA concentration profile, since one interface is closer to the source than the other. This asymmetry is maximized when one "end" of the droplet coincides with the source [maximal RNA concentration], i.e. when $d = R$. Thus, the 3D flow of droplets towards a point source matches physical intuition.

Flow of 2D droplets towards a Gaussian Source

The calculation above relies on many approximations: that the droplet maintains a round shape and its equilibrium concentration c_+ as it moves towards the source, interactions between c and m are weak and purely attractive, surface tension is negligible, and that production of m is independent of c. To test the validity of these approximations, we turn to phase field simulations of the full non-linear dynamics of m and c in 2D including surface tension κ. We take the simulation data from Ref. [8], which models the RNA-protein interactions via the terms $\chi cm + \gamma c^2 m^2$ in the free energy functional with $\chi < 0$ and $\gamma > 0$.

The simulated protein concentration field obeys conserved dynamics down the free energy hill. The simulated RNA concentration field obeys a reaction diffusion equation with a spatially localized RNA production rate $k_p(\boldsymbol{r}) = k_p e^{-(\boldsymbol{r}-d\hat{\boldsymbol{x}})^2/(2\sigma^2)}$. The DNA from which the RNA is transcribed has a Gaussian end-to-end distribution, and thus the variance σ^2 is a proxy for the size of the DNA locus. By thresholding the concentration field $c(\boldsymbol{x}, t)$ such that concentration values above $\Delta c/2$ are considered part of the dense phase, the authors locate the center of mass of the dense phase as the droplet centroid and then determine its velocity over time. They find that the droplet does not maintain a circular morphology but instead elongates and grows as it flows towards the source. Fig. 4b and c shows data from Pradeep Natarajan for the velocity and radius of the droplet as

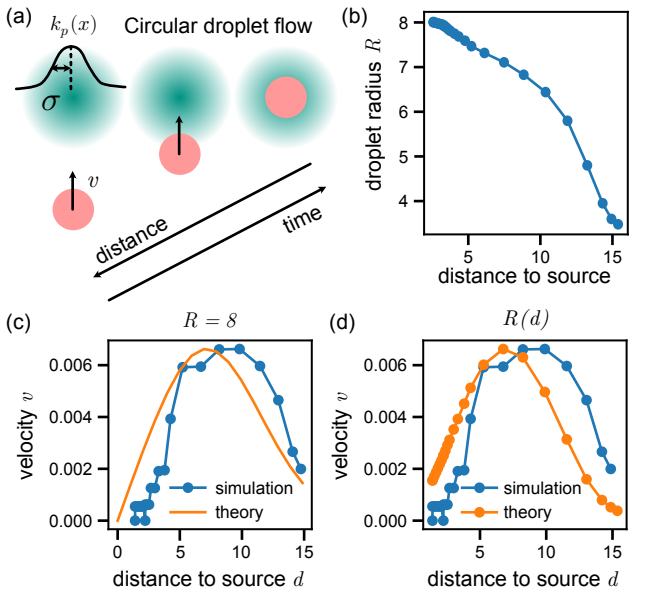

FIG. 4. (a) Flow of a circular protein droplet initialized at the origin towards a Gaussian RNA source with $\sigma = 4$ localized a distance $d_0 = 15.3$ away. (b) Droplet radius as a function of distance to source from phase field simulation data provided by Pradeep Natarajan [8]. (c, d) Velocity of droplet from simulation data compared to theoretical prediction [Eq. (19)] using a fixed droplet radius of $R = 8$ or the radius data in panel (b). Model parameters used in both simulations and calculations are $\chi = -1$, $c_+ = 0.7$, $c_- = 0.1$, $M_c = D = 1$, $k_D = 0.5$.

a function of distance to the source. The droplet grows with time both due to equilibrium coarsening and interactions with the RNA which promote accumulation of protein within the dense phase.

To compare our theoretical predictions to the simulated data, we calculate the self-propulsion velocity of a circular protein droplet in the linearized model in response to a Gaussian source of RNA production. We again employ the sharp interface approximation for c such that

$$c_q = \int d^2\boldsymbol{z} c(\boldsymbol{z}) e^{-i\boldsymbol{q}\cdot\boldsymbol{z}} = c_- \frac{\delta(q)}{2\pi q}(2\pi)^2 + \Delta c f(q), \quad (17)$$

where

$$f(q) = \int_0^{2\pi}\int_0^R dr r e^{iqr\cos\phi} = \frac{2\pi R}{|q|}J_1(R|q|). \quad (18)$$

Here, $f(0)$ is the area of the circular droplet and $J_1(x)$ is a Bessel function of the first kind. Substituting into the self consistency relation [Eq. (11)] and carrying out the 2D integrals in $\boldsymbol{q}$ and $\boldsymbol{r}$ gives the self-propulsion velocity in 2D:

$$v = -\frac{2M_c\chi}{c_+(\pi R^2)}\oint m(R,\phi)\cos\phi, \quad (19)$$

where the integral is now over the circular contour of the droplet, with integration measure $Rd\phi$. Comparing Eqs. (19) and (14), it is evident that the numerical prefactor for the velocity is just the dimension and is inversely proportional to the number of molecules in the dense phase c_+V_d where V_d is the d-dimensional volume of the droplet.

Although the RNA profile changes with time in the simulations, for our calculations we again assume that it is the steady state solution to the inhomogeneous Helmholtz equation. The solution is a convolution of the the Gaussian production rate $k_p(\boldsymbol{r})$ centered at a location $d\hat{\boldsymbol{x}}$ and the Green's function $G(\boldsymbol{r}-\boldsymbol{r}')$, which is the solution to the Helmholtz equation with a point source. That is,

$$m(\boldsymbol{r}) = \frac{k_p c_-}{2\pi D}\int d^2\boldsymbol{r}' G(\boldsymbol{r}-\boldsymbol{r}')e^{-\frac{(\boldsymbol{r}'-d\hat{\boldsymbol{x}})^2}{2\sigma^2}}, \qquad (20)$$

where the Green's kernel is a modified Bessel function of the second kind, $K_0(|\boldsymbol{r}-\boldsymbol{r}'|/\ell)$. Since Eq. (20) does not have a closed form expression, we numerically integrate Eq. (19) to obtain the self-propulsion velocity as a function of distance to the Gaussian source.

In Fig. 4, we compare our theoretical calculations for a constant radius of $R = 8$ using the same parameters as in the simulation. The theory curve is a zero-parameter fit with only the height of the curve rescaled to match the maximum simulated flow velocity. We find that the theory predics the non-monotic behavior of the velocity with distance to the source, and also captures the width and shape of the simulated curve, although more data for larger distances would be needed to make a more quantitative comparison. We also tried using the simulated values of droplet radius as a function of distance to the source $R(d)$ in Eq. (19), but did not see much improvement in the fit. In both cases, the theory overestimates the velocity for $d < R$ and underestimates the velocity for $d > R$. At short distances, the RNA production rate will be enhanced by the protein droplet and the re-entrant effect may thus slow the droplet down in the simulations relative to the lienearized calculations. Nonetheless, the success of the theory suggests that even in the nonlinear system, gradients in RNA concentration may be driving droplet motion.

In conclusion, we studied a non-equilibrium system of conserved proteins which produce RNA and investigated under what conditions protein droplets display directed motion. From our 1D analysis, we found that the steady state concentration profiles are maintained by a balance of reactive and diffusive fluxes. Asymmetry in the RNA profile at the two interfaces of the 1D droplet drives droplet flow, as long as the relative mobility of the protein or the relative production exceeds a critical threshold. We also considered droplet flow in response to localized production of RNA in 2D and 3D and found a non-monotonic relationship between the flow velocity and the distance to the source. Our theory suggests that RNA gradient sensing could be a mechanism by which transcription-associated condensates flow and interact within the nucleus.

[1] L. Demarchi, A. Goychuk, I. Maryshev, and E. Frey, Phys. Rev. Lett. **130**, 128401 (2023).

[2] Y. Shin and C. P. Brangwynne, Science **357**, eaaf4382 (2017).

[3] S. F. Banani, H. O. Lee, A. A. Hyman, and M. K. Rosen, Nature reviews Molecular cell biology **18**, 285 (2017).

[4] B. R. Sabari, A. Dall'Agnese, A. Boija, I. A. Klein, E. L. Coffey, K. Shrinivas, B. J. Abraham, N. M. Hannett, A. V. Zamudio, J. C. Manteiga, *et al.*, Science **361**, eaar3958 (2018).

[5] C. A. Weber, D. Zwicker, F. Jülicher, and C. F. Lee, Reports on Progress in Physics **82**, 064601 (2019).

[6] D. Zwicker, A. A. Hyman, and F. Jülicher, Physical Review E **92**, 012317 (2015).

[7] D. Zwicker, R. Seyboldt, C. A. Weber, A. A. Hyman, and F. Jülicher, Nature Physics **13**, 408 (2017).

[8] H. H. Schede, P. Natarajan, A. K. Chakraborty, and K. Shrinivas, bioRxiv (2022), 10.1101/2022.09.19.508534.

[9] S. Michelin, Annual Review of Fluid Mechanics **55**, 77 (2023).

[10] J. Kim, K. Y. Han, N. Khanna, T. Ha, and A. S. Belmont, Journal of cell science **132**, jcs226563 (2019).

[11] J. E. Henninger, O. Oksuz, K. Shrinivas, I. Sagi, G. LeRoy, M. M. Zheng, J. O. Andrews, A. V. Zamudio, C. Lazaris, N. M. Hannett, *et al.*, Cell **184**, 207 (2021).